

1 **Complexity of Frictional Interfaces: A Complex Network Perspective**

2 H. O. Ghaffari¹

3 *Department of Civil Engineering and Lassonde Institute, University of Toronto, Canada*

4 M. Sharifzadeh

5 Faculty of Engineering, Kyushu University, Hakozaki, Japan

6 E. Evgin

7 *Department of Civil Engineering, University of Ottawa, Ontario, Canada*

8 **Abstract:** The shear strength and stick-slip behavior of a rough rock joint are analyzed using the
9 complex network approach. We develop a network approach on correlation patterns of void
10 spaces of an evolvable rough fracture (crack type II). Correlation among networks properties
11 with the hydro -mechanical attributes (obtained from experimental tests) of fracture before and
12 after slip is the direct result of the revealed non-contacts networks. Joint distribution of locally
13 and globally filtered correlation gives a close relation to the contact zones attachment-
14 detachment sequences through the evolution of shear strength of the rock joint. Especially spread
15 of node's degree rate to spread of clustering coefficient rate yielded possible stick and slip
16 sequences during the displacements. Our method can be developed to investigate the complexity

¹ h.o.ghaffari@gmail.com;

hamed.owladeghaffari@utoronto.ca

Dept. Civil Engineering, U of T, MB108-170 College Street-Toronto-ON-Canada

17 of stick-slip behavior of faults as well as energy /stress localization on crumpled shells/sheets in
18 which ridge networks are controlling the energy distribution.

19 **Key words**: Frictional interface; Rock *joint*, *Shear strength*, *Stick-slip*, *Complex networks*,
20 *Correlation*, *Contact areas*

21 **1. Introduction**

22 During the last decade, complex networks have been used increasingly in different fields
23 of science and technology [1-3]. Initial applications of complex networks in geosciences were
24 mostly related to earthquakes [4-6]. Characterization of spatial and temporal structural
25 complexity of such recursive events has been the main objective of the related research [7-13].
26 Understanding of spatio-temporal topological complexity of events based on field
27 measurements can disclose some other facets of these intra/extra woven events.

28 Studies pertaining to the topological complexity and its application in some geoscience
29 fields reveals that acquisition and gathering of direct information (especially in temporal scale) is
30 difficult and in many cases are (were) impossible (at least with current technologies). In addition
31 to complex earthquake networks, recently the analysis of climate networks, volcanic networks,
32 river networks and highway networks, as the large scale measurements, have been taken into
33 account [9-13]. In small scales, topological complexity has been evaluated in relation to
34 geoscience fields such as the gradation of soil particles, fracture networks, aperture of fractures,
35 and granular materials [14-20]. The initial step refers to organizational step which tries to find
36 out possible dominant well-known structures within the system. Next step in the most of the
37 mentioned works is to provide a suitable and simple method to yield a similar structure. Such
38 algorithm may support the evolution of structure in spatial or/and temporal cases [21].

39 May be the most important structural complexity in geological fields is related to fracture
40 networks. Fracture networks with dilatancy [22], joint networks in excavation damaged zones,
41 cracking in pavements (or other natural/man-made structures) and fault networks in large scale
42 have been recognized [23-25]. In the analysis of these networks, the characterization of fractures
43 in a proper space such as friction-displacement space is an essential step. Furthermore, with
44 taking the direct relationship between void spaces and contact areas in to account, one may
45 interest in considering the induced topological complexity of the opening elements (non-
46 frictional contacts) into the fracture behavior. Using linear elastic fracture mechanics, we know
47 aperture or aspect ratio is generally the index to available energy in growth of rupture. Crack
48 like behavior of rupture in frictional interfaces also support the role of contact areas and
49 equivalently apertures. In addition, the variations of fluid flow features (such as permeability
50 and tortuosity) directly are controlled with aperture spaces. In order to characterize the main
51 attributes of the fractured systems, e.g. mechanical and hydraulic properties, several methods
52 have been suggested in the literature [26-30]. Recently, the authors have proposed the
53 implementation of a complex network analysis for the evolution of micro-scale apertures in a
54 rough rock fracture [18-19]. Based on a Euclidean measure, the results confirmed the
55 dependency of hydro-mechanical properties to the attributes of characterized aperture networks.
56 The present study is also related to the complex aperture networks. However, the current study
57 presents the analysis of frictional forces during shearing based on the *correlation* of apertures in
58 a rock joint. The analysis is associated with set up a network on an attribute (such as aperture
59 distribution) in an area. The aforementioned method has also been employed in the analysis of
60 the coupled partial differential equations which was related to two-phase flow [31].

61 With respect to avalanche-like behavior of collective motion of the ensemble discrete
62 contacts (in the vicinity of a phase transition step), we try to characterize the collective behavior
63 of aperture strings using networks. In this paper we will answer the following three questions: 1)
64 Is there any (hidden) complex structure in the experimentally observed apertures? 2) What is the
65 effect of specific structural complexity of apertures on mechanical response of a fracture? 3)
66 How do apertures regulate with each other to show well-known slip-friction curve? In other
67 words, can we relate the topological complexity of apertures to the evolution path of the
68 fracture?

69 The organization of the paper is as follows: Section 2 includes a brief description of
70 networks and their characterization. In addition, the construction procedure of aperture networks
71 is explained. Section 3 covers a summary of the experimental procedure. The last section
72 presents the evaluation of the pre- and post-peak (stick-slip) behavior of a rock joint which is
73 followed by the analysis of the constructed network.

74

75 **2. Network of Evolving Apertures**

76

77 In this section we describe a general method of setting up a network on a fracture surface
78 while the surface property is a superposition of very narrow profiles (ribbons) of one attribute of
79 the system. In other words, one attribute of the system is “granulated “over strings (profiles or
80 ribbons). The relationship between the discrete strings –inferred from long range correlation or
81 elastic forces- results an interwoven network, i.e., topological complexity of interactions. The
82 frictional behavior including the stick-slip response of a joint is related to the sum of real contact
83 areas, which fluctuates with the changes in apertures. It also occurs based on the collective

84 motion and spatially coupled of contact zones. It is shown that the structural complexity of the
 85 dynamic aperture changes is controlling and regulating the joint behavior and its unstable
 86 response. In order to explain the details of our work, we need to characterize the topological
 87 complexity.

88 A network consists of nodes and edges connecting the [32]. To set up a nondirected
 89 network, we considered each string of measured aperture as a node. Each aperture string has N
 90 pixels where each pixel shows the void size of that cell. Depending on the direction of strings,
 91 the length of the profiles varies. The maximum numbers of strings (in our cases) are in the
 92 perpendicular direction to the shear, while the minimum one is in the parallel direction. To make
 93 an edge between two nodes, a correlation measurement (C_{ij}) over the aperture profiles was
 94 used. The main point in the selection of each space is to explore the explicit or implicit hidden
 95 relations among different distributed elements of a system. For each pair of signals (profiles) V_i
 96 and V_j , containing N elements (pixels) the correlation coefficient can be written as [33]:

$$97 \quad C_{ij} = \frac{\sum_{k=1}^N [V_i(k) - \langle V_i \rangle] \cdot [V_j(k) - \langle V_j \rangle]}{\sqrt{\sum_{k=1}^N [V_i(k) - \langle V_i \rangle]^2} \cdot \sqrt{\sum_{k=1}^N [V_j(k) - \langle V_j \rangle]^2}} \quad (1)$$

98 where $\langle V_i \rangle = \frac{\sum_{k=1}^N V_i(k)}{N}$. Obviously, It should be noted that C_{ij} is restricted to $-1 \leq C_{ij} \leq 1$, where
 99 $C_{ij}=1$, 0, and -1 are related to perfect correlations, no correlations and perfect anti-correlations,
 100 respectively.

101 Selection of a threshold (ξ) to make an edge, can be seen from different views.
 102 Choosing a constant value may be associated with the current accuracy of accumulated data

103 where after a maximum threshold the system loses its dominant order. In fact, there is not any
104 unique way in the selection of a constant value, however, preservation of the general pattern of
105 evolution must be considered while the hidden patterns can be related to the several characters of
106 the network. These characters can express different facets of the relations, connectivity,
107 assortivity (hubness), centrality, grouping and other properties of nodes and/or edges [34-36].
108 Generally, it seems obtaining stable patterns of evolution (not absolute) over a variation of ξ can
109 give a suitable and reasonably formed network [33]. Also, different approaches have been used
110 such as density of links, the dominant correlation among nodes, c - k space and distribution of
111 edges or clusters. In this study, we set $C_{ij} \geq \xi = 0.2C_{ij}^{\max}$. Considering with this definition, we are
112 filtering uncorrelated profiles over the metric space. In the previous study, the sensitivity of the
113 observed patterns (associated with the Euclidean distance of profiles) has been distinguished
114 [18].

115 The clustering coefficient describes the degree to which k neighbors of a particular node
116 are connected to each other. What we mean by neighbors is the connected nodes to a particular
117 node. The clustering coefficient shows the collaboration between the connected nodes. Assume
118 that the i^{th} node to have k_i neighboring nodes. There can exist at most $k_i(k_i - 1)/2$ edges
119 between the neighbors. We define C_i as the ratio

$$120 \quad c_i = \frac{\text{actual number of edges between the neighbors of the } i^{\text{th}} \text{ node}}{k_i(k_i - 1)/2} \quad (2)$$

121 Then, the clustering coefficient is given by the average of C_i over all the nodes in the
122 network [21]:

123
$$C = \frac{1}{N} \sum_{i=1}^N c_i. \quad (3)$$

124 For $k_i \leq 1$ we define $C \equiv 0$. The closer C is to one the larger is the interconnectedness
 125 of the network. The connectivity distribution (or degree distribution), $P(k)$, is the probability of
 126 finding nodes with k edges in a network. In large networks, there will always be some
 127 fluctuations in the degree distribution. The large fluctuations from the average value ($\langle k \rangle$)
 128 refers to the highly heterogeneous networks while homogeneous networks display low
 129 fluctuations [21]. From another perspective, clustering in networks is closely related to degree
 130 correlations. Vertex degree correlations are the measures of the statistical dependence of the
 131 degrees of neighbouring nodes in a network [35]. Two-point correlation is the criterion in
 132 complex networks as it can be related to network assortativity.

133 The concept of two-point correlation can be included within the conditional probability
 134 distribution $P(k' | k)$ that a node of degree k is connected to a node of degree k' . In other words,
 135 the degrees of neighbouring nodes are not independent. The meaning of degree correlation can
 136 also be defined by the average degree of nearest neighbours ($\langle k_{nn} \rangle_k$). If $\langle k_{nn} \rangle_k$ increases with
 137 k high degree nodes (hubs) tend to make a link to high degree nodes, otherwise, if
 138 $\langle k_{nn} \rangle_k$ decreases with k , high degree nodes (hubs) tend to make a link with low degree nodes
 139 (disassortative) [34-36]. From the point of view of fractal complex networks [37-38], the degree
 140 correlation may be used as a tool to distinguish the self-similarity of network structures. In fact,
 141 in fractal networks large degree nodes (hubs) tend to connect to small degree nodes and not to
 142 each other (fractality and disassortativity). Also, the clustering nature of a network can be drawn
 143 as the average over all nodes of degree k giving a clustering distribution (or spectrum). In many

144 real-world networks such as the internet the clustering spectrum is a decreasing function of
145 degree which may be interpreted as the hierarchical structures in a network. In contrast, some
146 other networks such social networks and scientific collaborations (and also we will see complex
147 aperture networks) are showing assortative behaviour [35]. It will be shown that spreading of
148 crack like behaviour due to shearing a fracture, can be followed with the patterns of proper
149 spectrum. Similarly, by using the degree correlation, one may define the virtual weight of an
150 edge as an average number of edges connected to the nodes [39].

151 The average (characteristic) path length L is the mean length of the shortest paths
152 connecting any two nodes on the graph. The shortest path between a pair (i, j) of nodes in a
153 network can be assumed as their geodesic distance, g_{ij} , with a mean geodesic distance L given as
154 below [2, 21]:

$$155 \quad L = \frac{2}{N(N-1)} \sum_{i < j} g_{ij}, \quad (4)$$

156 where g_{ij} is the geodesic distance (shortest distance) between node i and j , and N is the number
157 of nodes. We will use a well known algorithm in finding the shortest paths presented by Dijkstra
158 [40]. Based on the mentioned characteristics of networks two lower and upper bounds of
159 networks can be recognized: regular networks and random networks (or Erdős–Rényi networks
160 [41]). Regular networks have a high clustering coefficient ($C \approx 3/4$) and a long average path
161 length. Random networks (construction based on random connection of nodes) have a low
162 clustering coefficient and the shortest possible average path length. However Watts and Strogatz
163 [42] introduced a new type of networks with high clustering coefficient and small (much smaller
164 than the regular ones) average path length. This is called small world property.

165 **3. Summary of Laboratory Tests**

166 To study the small world properties of rock joints, the results of several laboratory tests
167 were used. The joint geometry consisting of two joint surfaces and the aperture between these
168 two surfaces were measured. The shear and flow tests were performed later on. The rock was
169 granite with a unit weight of 25.9 kN/m^3 and uniaxial compressive strength of 172 MPa. An
170 artificial rock joint was made at mid height of the specimen by splitting and using special joint
171 creating apparatus, which has two horizontal jacks and a vertical jack [43-44]. The sides of the
172 joint are cut down after creating the joint. The final size of the sample is 180 mm in length, 100
173 mm in width and 80 mm in height. Using special mechanical units, various mechanical
174 parameters of this sample were measured. A virtual mesh having a square element size of 0.2
175 mm was spread on each surface and the height at each position was measured by a laser scanner.
176 The details of the procedure can be found in [45-46]. Different cases of the normal stress (1,
177 3 and 5 MPa) were used while the variation of surfaces were recorded. **Figure 1** shows the shear
178 strength evolution under different normal loads. In this study, we focus on the patterns, obtained
179 from the test with a 3 MPa normal stress.

180 **4. Implementation and Analysis of Complex Aperture Networks**

181 In this section we set up the designated complex network over the aperture profiles,
182 which are perpendicular to the shear direction. By using the correlation measure, the distribution
183 of correlation values along profiles and during the successive shear displacements were obtained
184 (**Fig. 2**). Plotting the correlation distribution shows the transition from a near Poisson distribution
185 to a Gaussian distribution. The change in the type of distribution is followed by the phenomena
186 of the tailing, which is inducing the homogeneity of the correlation values towards high and anti-

187 correlation values. In other words, tailing procedure is tied with the quasi-stable (residual part)
188 states of the joint. Thus, this can be described by reducing the entropy of the system where the
189 clusters of information over correlation space are formed. From another point of view, with
190 considering the correlation patterns, it can be inferred that throughout the shear procedure, there
191 is a relatively high correlation between each profile and the profiles at a certain neighborhood
192 radius. This radius of correlation is increasing non-uniformly (anisotropic development) during
193 shear displacement (Fig.3).

194 By using the method described in the previous section, a complex aperture network is
195 developed from the correlation patterns (Fig.4). As it can be seen in this figure, the formation of
196 highly correlated nodes (clusters) is distinguishable near the peak point. It can be estimated that
197 the controlling factor in the evolution path of the system is related to the formation of cliques
198 (communities). We will show locality properties of the clusters (intera structures) are much
199 more discriminated at last displacements rather than initial time steps while global variations of
200 the structures are more sensitive to reduction in the shear stress. In fact, forming hubs in the
201 constructed networks may give the key element of synchronization of aperture profiles (or
202 collective motion of discrete contact zones) along the shear process. In other words, reaching to
203 one or multiple attractors and the rate of this reaching after peak point are organized by the
204 spreading and stabilizing the clusters. Unfortunately, due to a low rate of data sampling, the
205 exact evolution of patterns before peak-point is not possible. However, during the discussion on
206 the joint degree correlations, a general concept will be proposed.

207 The three well-known characteristics of the constructed networks, namely total degree of
208 nodes, clustering coefficient and mean shortest path length are depicted as a function of shear
209 displacement in Figure 5. As it can be followed there is a nearly monotonic growth/decay of the

210 parameters. A considerable sharp change in transition from shear displacement 1 to 2 mm is
211 observed for all three illustrated parameters. This transition is assumed as state transition from
212 the pre-peak to post peak state, while with taking into account the rate of the variation of the
213 parameters the transformation step is discriminated. Also, despite of clustering coefficient trend
214 which show a fully-growth shape the number of edges and mean short length after a shear
215 displacement of 12 mm roughly exhibiting a quasi-stable trend. These results provide the
216 necessary information for the classification of the aperture networks in our rock joint. The high
217 clustering coefficient and low average (characteristic) path length clearly show that our aperture
218 networks have small-world properties.

219 The development of shear stress over the networks is much faster after the peak point
220 than the pre-peak states. This feature can be explained by understanding the concept of the net-
221 contact areas [59]. At interlocking of asperities step-before maximum static friction- the two-
222 point correlation shows a relatively more uniform shape rather than former and later cases. Also,
223 the current configuration implies that the homogeneity of the revealed network where the nodes
224 with high degree are tending to absorb nodes with low edges. This indicates the property of self-
225 similarity within the network structures. The shear displacements immediately after or near peak
226 (Figure 6) point destroy the homogeneity of the network and spreading slow fronts and dropping
227 of the frictional coefficient is accompanied with a trial to make stable cliques, inducing the
228 heterogeneity to the network structures. Using a microscopic analysis, it can be proven that, for
229 homogenous topologies, many small clusters spread over the network and merge together to
230 form a giant synchronized cluster [54-56]. This event is predicted before reaching to the peak
231 threshold. In heterogeneous graphs, however, one or more central cores (hubs) are driving the
232 evolutionary path and are figuring out the synchronization patterns by absorbing the small

233 clusters. As can be seen in Figure 6 and Figure 7, two giant groups are recognizable after 14 mm
234 displacement. This shows the attractors states in a dynamic system. However, two discriminated
235 clusters are not showing the self-similarity structures within the proper networks, i.e., hubs with
236 high degree nodes are separated from the hubs with low degree nodes. In general, one may
237 overestimate the self-similarity of internal structures of the networks, which means that in the
238 entire steps at least a small branch of fractility can be followed.

239 The attributed weight distribution, associated with the two-point correlation concept
240 (Fig.7) shows as if the virtual heaviness of edges are increasing, simultaneously, the joint degree
241 distribution is also growing, which indicates the networks are assortative. The distribution of the
242 weights from unveiled hubs also clearly can be followed in Figure 7 while two general
243 discriminated patterns are recognizable. On the contrary, if the patterns of correlation of
244 clustering coefficients are drawn (Fig.8), the eruption of local synchronization is generally closed
245 out after (or at least near) peak point while again during and after dropping shear strength, the
246 variation of local clusters will continue. Especially, at the point near to critical step, the local
247 clusters present much more uniform percolation rather than the other states while at final steps
248 the stable state (or quasi-stable) regime of regional structures is not clear. It is worth stressing the
249 rate of variation of local joint clustering patterns at apparently quasi-steps are much higher than
250 the global patterns, i.e., joint degree distribution. Also, it must be noticed that before peak point
251 the structures of joint triangles density is approximately unchangeable. Then as a conclusion,
252 burst of much dense local hubs is scaled with disclosing of slow fronts spreading.

253 Following the spectrum of the networks in a collective view (Fig.9) shows a nearly
254 uniform growing trend where a third degree polynomial may be fitted. However, with respect to
255 individual analysis (local analysis) of $c_i - k_i$, a negative trend can be pursued. The spectrum of

256 the networks can be related to three-point correlation concept which expresses the probability of
 257 selecting a node with a certain degree, so that it is connected to other two nodes with the definite
 258 degrees. The evolution of spectrum of aperture networks in a Euclidean space and using a
 259 clustering analysis on the accumulated objects has come out the details of the fracture evolution,
 260 either in the mechanical or hydro-mechanical analysis [18-19]. But, in our case, detecting such
 261 explicit scaling is difficult. Let us transfer all of the calculated network properties in a variation
 262 (rate) space (Fig.10). Depicting the clustering coefficient and mean degree rates, shows a similar
 263 trend with the evolution of shear strength, however, after 8 mm displacement the variation of
 264 edges and clustering coefficient unravels the different fluctuations.

265 The negative scaling (for large anisotropy) in $\frac{dc_i}{dt} - \frac{dk_i}{dt}$ space can be expressed by

266 $\frac{dk_i}{dt} \cong -800 \frac{dc_i}{dt} + 20$. As it can be followed in Figure 10, the congestion of objects makes a

267 general elliptic which approximately covers all of points where the details of the correlation
 268 among two components presents how the expansion and contraction of patterns fall into the final
 269 attractors (Fig.10). Thus, such emerged patterns related to the two-point correlation of variation
 270 rate of edges and rate of clustering coefficient are proposing a certain core in each time step so
 271 that the absorbing of objects within a “black hole” at residual part is much more obvious rather

272 than other states. With definition of anisotropy by $S = \frac{\sigma(\frac{d \langle k \rangle}{dt})}{\sigma(\frac{dC}{dt})}$ (σ is standard

273 deviation), the rate changes of profiles in a new space and with reference to the pre and post peak
 274 behaviours are obtained (Fig.11). Transferring from interlocking step to Coulomb threshold level
 275 is accompanying with the maximum anisotropy (Fig.11b) and immediate dropping and then

276 starting to fluctuate until reaching to a uniform decline. The fluctuation of anisotropy from 2mm
277 to 13 mm may be associated with the stick-slip behaviour of the rock joint as the main reason of
278 shallow earthquakes [57-58]. It should be noticed that the results of the later new space is
279 completely matching with the analysis of joint degree and joint clustering distribution. In **Figure**
280 **11.a**, we have illustrated a new variable with regard to durability and entropy of the system,
281 $\frac{dC}{dt} \times \frac{d \langle k \rangle}{dt}$. In fact with definition of such parameter the fluctuation in anisotropy is filtered
282 while initiating the post stick-slip behavior is scaled with the minus or zero variation of the
283 parameter. In [59-61], we analyzed the sub-graph structures and frequencies over parallel and
284 perpendicular aperture networks. Also, a directed network based on contact strings and
285 preferentiality of possible energy flow in rupture tips has been introduced. We also, inspected the
286 synchronization of strings using a Kuromoto model [59].

287 5. Conclusions

288 In this study, we presented a special type of complex aperture network based on
289 correlation measures. The main purpose of the study was to make a connection between the
290 apparent mechanical behavior of a rock joint and the characterized network. The incorporation of
291 the correlation of apertures and the evaluation of continuously changing contact areas (i.e.
292 growth of aperture) within the networks showed the effects of structural complexity on the
293 evolution path of a rock joint. Our results showed that the main characteristics of aperture
294 networks are related to the shear strength behavior of a rock joint. The residual shear strength
295 corresponded to the formation of giant groups of nodes in the networks. In addition, based on the
296 joint correlation upon edges and triangles, the pre-peak and post peak behaviour of a rock joint
297 under shear were analyzed. Our results may be used as an approach to insert the complex

298 aperture networks into the surface growth methods or general understanding of the conditions for
299 a sudden movement (shock) in a fault.

300

301 **References**

- 302 1. Newman M. E. J. The structure and function of complex networks, *SIAM Review* 2003;
303 45(2): 167- 256.
304
- 305 2. Dorogovetev S.N., Goltsev A.V.2008.Critical phenomena in complex networks .*Review*
306 *Modern Physics*.Vol.80.Oct-Dec.2008
307
- 308 3. Boccaletti S.,Latora V., Moreno Y.,Chavez M.,Hwang D-U.2006.Complex Networks :
309 Structure and Dynamics. *Physics Reports* 424,175-308
310
- 311 4. Abe S, Suzuki N.2006. Complex network description of seismicity. *Nonlin process*
312 *Geophys*;13:145-150
313
- 314 5. Jim´enez A, Tiampo K.F., Posadas A.M., Luz´on F., and Donner R. Analysis of complex
315 networks associated to seismic clusters near the Itoiz reservoir dam. *Eur. Phys. J. Special*
316 *Topics* 2009; 174, 181–195.
317
- 318 6. Baiesi M, Paczuski M. 2004.Scale free networks of earthquakes and aftershocks. *Physical*
319 *review E* 2004; 69 (2): 066106.1-066106.8
320
- 321 7. Doering R.C.1991.*Modeling Complex Systems: Stochastic processes, Stochastic Differential*
322 *Equations, and Fokker-Planck Equations*; 1990 Lectures in complex systems, SFI Studies in
323 the science of complexity.
324
- 325 8. Ghaffari H.O., Sharifzadeh M Shahriar , K. & Pedrycz W. Application of soft granulation
326 theory to permeability analysis , *International Journal of Rock Mechanics and Mining*
327 *Sciences*, Volume 46, Issue 3, 2009, Pages 577-589
328
- 329 9. Tsonis, A. A., and P. J. Roebber. 2003. The architecture of the climate network. *Physica*,
330 333A, 497–504.
- 331 10. Xie F, Levinson D. Topological evolution of surface transportation networks. *Computers,*
332 *Environment and Urban Systems* 33 (2009) 211–223
333
- 334 11. Tsonis, A.A. and Swanson, K. L.2008. Topology and Predictability of El Niño and La Niña
335 Networks. *Physical Review Letters* 100, 228502 (2008)
336

- 337 12. Bartolo S.D, Dell'Accio F, and Veltri M.2009. Approximations on the Peano river network:
 338 Application of the Horton-Strahler hierarchy to the case of low connections, *Phys. Rev. E* 79,
 339 026108 (2009).
 340
- 341 13. Latora V., Marchiori M. 2002, Is the Boston subway a small-world network? *Physica A*, 314,
 342 109-113.
 343
- 344 14. Mooney S.J, Dean K. Using complex networks to model 2-D and 3-D soil porous
 345 architecture. *Soil Sci Soc Am J* 73:1094-1100 (2009)
 346
- 347 15. Perez-Reche F, Taraskin S.N, Neri F.M, Gilligan C.A.2009.Biological invasion in soil
 348 :complex network analysis . Proceedings of the 16th international conference on Digital
 349 Signal Processing, Santorin, Greece .2009.
 350
- 351 16. Karabacak T, Guclu H, Yuksel M. Network behaviour in thin film growth dynamics. *Phys.*
 352 *Rev. B* 79, 195418 (2009) – Published May 15, 2009
- 353 17. Valentini L Perugini D, Poli G. The small-world topology of rock fracture networks. *Physica*
 354 *A* 2007; 377:323–328.
 355
- 356 18. Ghaffari H.O., Sharifzadeh M. & Fall M. Analysis of Aperture Evolution in a Rock Joint
 357 Using a Complex Network Approach; *International Journal of Rock Mechanics and Mining*
 358 *Sciences*, Volume 47, Issue 1, January 2010, Pages 17-29.
 359
- 360 19. Ghaffari H.O., Sharifzadeh M. ,Evgin E; Complex Aperture Networks.
 361 <http://aps.arxiv.org/abs/0901.4413>
 362
- 363 20. Walker D.M, Tordesillas A. Topological evolution in dense granular materials: a complex
 364 networks perspective. *International Journal of Solids and Structures* 47, 2010, 624-639.
 365
- 366 21. Albert R., Barabasi A.-L. Statistical mechanics of complex networks. *Review of Modern*
 367 *Physics*; 74,2002, 47–97.
 368
- 369 22. Alkan H. Percolation model for dilatancy-induced permeability of the excavation damaged
 370 zone in rock salt, *International Journal of Rock Mechanics and Mining Sciences*, 46(4),
 371 2009, Pages 716-724.
 372
- 373 23. Adler MP and Thovert JF. Fractures and fracture networks. Kluwer Academic; 1999.
 374
- 375 24. Alava M. J , Nukala P.K. V. V.; Zapperi S, Statistical models of fracture , *Advances in*
 376 *Physics*, Volume 55, Issue 3 , 2006 , pages 349 – 476.
 377

- 378 25. Knopoff, L. The organization of seismicity on fault networks, *PNAS* April 30, 1996 vol. 93
379 no. 9 3830-3837.
380
- 381 26. R.W. Zimmerman, D.W. Chen and N.G.W. Cook, The effect of contact area on the
382 permeability of fractures, *J Hydrol* 139 (1992), pp. 79–96.
383
- 384 27. Lanaro F.A. Random field model for surface roughness and aperture of rock fractures. *Int J*
385 *Rock Mech Min Sci*, 2000, 37:1195-1210.
386
- 387 28. Brown SR, Kranz RL , Bonner BP. Correlation between the surfaces of natural rock joints,
388 *Geophys Res Lett*, 1986; 13(13):1430-1433.
389
- 390 29. Hakami E, Einstein H H, Genitier S , Iwano M. Characterization of fracture apertures-
391 methods and parameters. In: *Proc of the 8th Int Congr on Rock Mech*, Tokyo, 1995: 751-754.
392
- 393 30. Lanaro F, Stephansson O.A. Unified model for characterization and mechanical behavior of
394 rock fractures. *Pure Appl Geophys*, 2003; 160:989-998
395
- 396 31. Ghaffari H. O, Complexity Analysis of Unsaturated Flow in Heterogeneous Media Using a
397 Complex Network Approach, <http://arxiv.org/ftp/arxiv/papers/0912/0912.4991.pdf>
398
- 399 32. Wilson RJ. *Introduction to Graph Theory*. Fourth Edition: Prentice Hall, Harlow, 1996.
- 400 33. Gao Z. and Jin N. Flow-pattern identification and nonlinear dynamics of gas-liquid two-
401 phase flow in complex networks; 2009. *Physical Review E* 79, 066303.
402
- 403 34. Newman M.E.J. Assortative mixing in networks. *Phys. Rev. Lett.* 89, 208701 (2002).
404
- 405 35. R. Xulvi-Brunet and I.M. Sokolov. Changing correlations in networks: assortativity and
406 dissortativity. *Acta Phys. Pol. B*, 36, 1431 (2005).
407
- 408 36. Colizza, V., Flammini, A., Serrano, M.A., Vespignani, A. Detecting rich-club ordering in
409 complex networks, *Nature Physics* 2, Issue 2, 2006, Pages 110-115 .
410
- 411 37. Song C, Havlin S, Makse HA., Origins of fractality in the growth of complex networks,
412 *Nature Physics* 2, 275 - 281 (2006), pages 275-281.
413
- 414 38. Kim JS, Goh KI, Salvi G, Oh E, Kahng B, Kim D, Fractality in complex networks: Critical
415 and supercritical skeletons, *Phys. Rev. E* 75, 016110 (2007).
416

- 417 39. Korniss G, Synchronization in weighted uncorrelated complex networks in a noisy
418 environment: Optimization and connections with transport efficiency, *Phys. Rev. E* 75,
419 051121 (2007).
420
- 421 40. Dijkstra EW, A note on two problems in connexion with graphs, *Numerische mathematik*,
422 1959 ,pp. 269-271.Springer
423
- 424 41. Newman M., Barabasi A-L., Watts D.J.*The Structure and Dynamics of Networks*.2006.
425 Princeton University Press
426
- 427 42. Watts DJ, Strogatz SH. Collective dynamics of small-world networks. *Nature* ,1998;
428 393:440-442
429
- 430 43. Mitani, Y., Esaki, T., Zhou, G., Nakashima, Y. Experiments and simulation of Shear – Flow
431 Coupling properties of rock joint. In: Proc., 39th Rock mechanics conference: Glückauf,
432 Essen, (2003), 1459–1464.
433
- 434 44. Mitani, Y., Esaki, T., Sharifzadeh, M., Vallier, F. Shear – Flow coupling properties of rock
435 joint and its modeling Geographical Information System (GIS). In: Proc., 10th ISRM
436 Conference, South African Institute of Mining and Metallurgy, (2003), 829–832.
437
- 438 45. Sharifzadeh M. Experimental and theoretical research on hydro-mechanical coupling
439 properties of rock joint. Ph.D. thesis, Kyushu University, Japan; 2005.
440
- 441 46. Sharifzadeh M, Mitani Y, Esaki T .Rock joint surfaces measurement and analysis of aperture
442 distribution under different normal and shear loading using GIS, *Rock Mechanics and Rock*
443 *Engineering*, Volume 41, Number 2 / April, 2008, Pages 299-323.
444
- 445 47. L. Valentini, D. Perugini and G. Poli, The ‘small-world’ nature of fracture/conduit
446 networks:next term Possible implications for disequilibrium transport of magmas beneath
447 mid-ocean ridges, *Journal of Volcanology and Geothermal Research* 159 (2007), pp. 355–
448 365.
449
- 450 48. Gnecco, Enrico; Meyer, Ernst, *Fundamentals of Friction and Wear*, 2007, Springer, 714 p.
451
- 452 49. Rubinstein, S., Cohen, G. & Fineberg, J. Contact area measurements reveal loading-history
453 dependence of static friction. *Phys. Rev. Lett.* 96, 256103 (2006)
454

455 50. Xia, K., Rosakis, A. J. & Kanamori, H. Laboratory earthquakes: the sub-Raleigh-to-
456 supershear rupture transition. *Science* 303, 1859–1861 (2004)
457

458 51. Rubinstein, S. M., Cohen, G. & Fineberg, J. Detachment fronts and the onset of dynamic
459 friction. *Nature* 430, 1005–1009 (2004)
460

461 52. S. M. Rubinstein, G. Cohen, and J. Fineberg, Visualizing Stick-Slip: Experimental
462 observations of processes governing the nucleation of frictional sliding, *J. Phys. D: Appl.*
463 *Phys.* 42 214016, (2009).
464

465 53. Sornette D, *Critical Phenomena in Natural Sciences*, Springer-Verlag Berlin Heidelberg,
466 2006.
467

468 54. Arenas A., Diaz-Guilera A., Kurths J., Moreno Y., Zhou C. Synchronization in complex
469 networks *.Physics Reports* ,2008, 469,93-153.
470

471 55. Strogatz,S.H. Exploring complex networks, *Nature*. 2001; Vol .410:268-276.
472

473 56. Barahona M, and Pecora L. M. Synchronization in Small-World Systems, *Phys. Rev. Lett.*
474 89, 054101 (2002)
475

476 57. Brace WF, Byerlee JD, Stick-slip as a mechanism for earthquakes, *Science*, Volume 153,
477 Issue 3739, pp. 990-992.
478

479 58. Scholz CH, Earthquakes and friction laws, *Nature*, 391, 37-42 (1998).
480

481 59. H.O.Ghaffari and R.P.Young, ArXive-prints (2011) <http://arxiv.org/abs/1105.4265>.
482

483 60. H.O.Ghaffari, A.Nabovati, M. Sharifzadeh, and R.P.Young, <http://arxiv.org/abs/1103.1124>.
484

485 61. H.O.Ghaffari and R.P.Young, Motifs of Networks from Shear Fractures; submitted to Journal
486

487

488

489

490

491

492

493

494

495

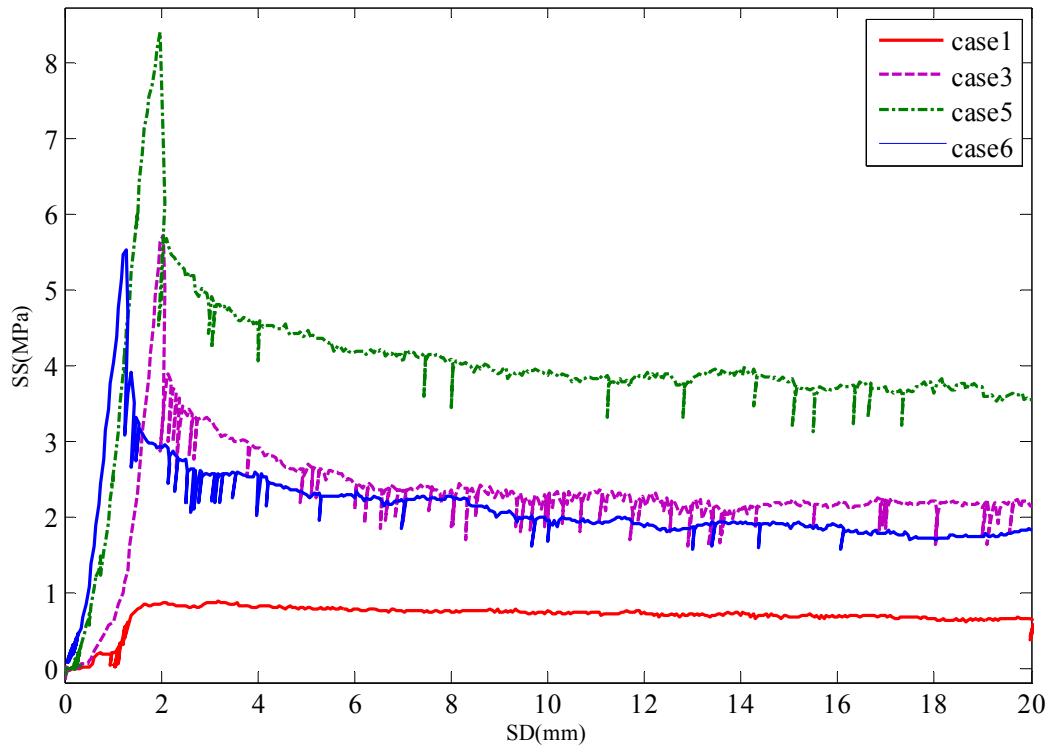
496

497

498

Figures

499



500

501 FIGURE 1. Variation of shear strength for different cases (normal stresses for
 502 case1:1mpa, case3: 3 MPa, case5: 5 MPa and case6: 3 MPa (without control of upper
 503 shear box) [46].

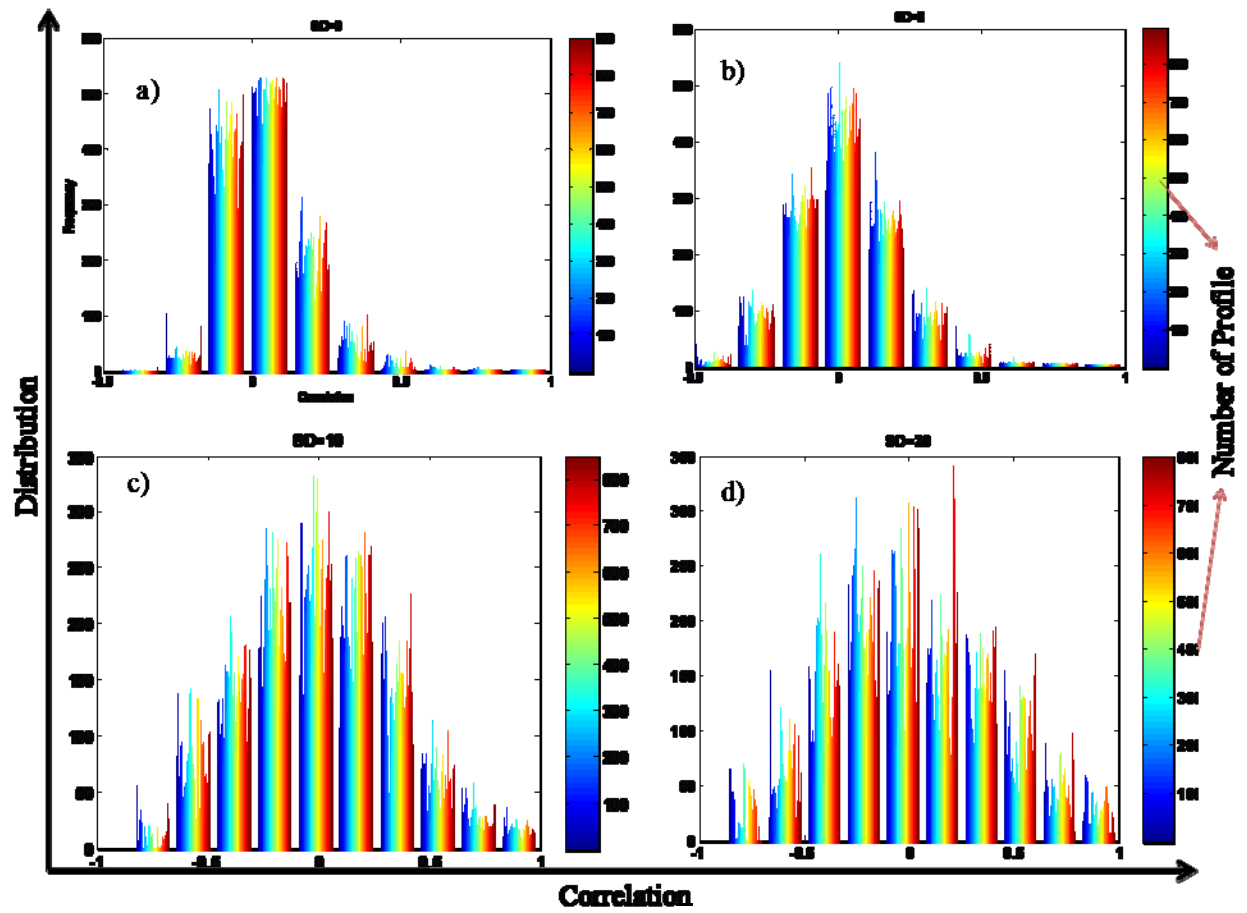
504

505

506

507

508

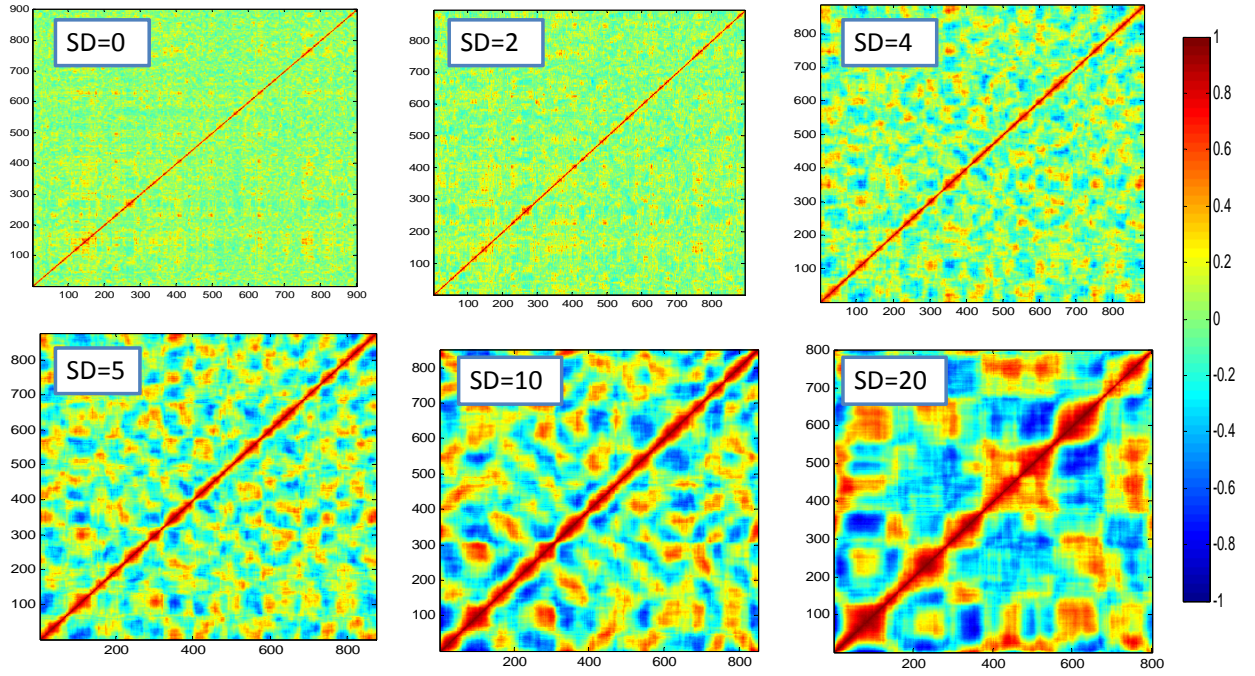


509

510 FIGURE 2. Evolution of correlation values of aperture profiles at shear displacement s :

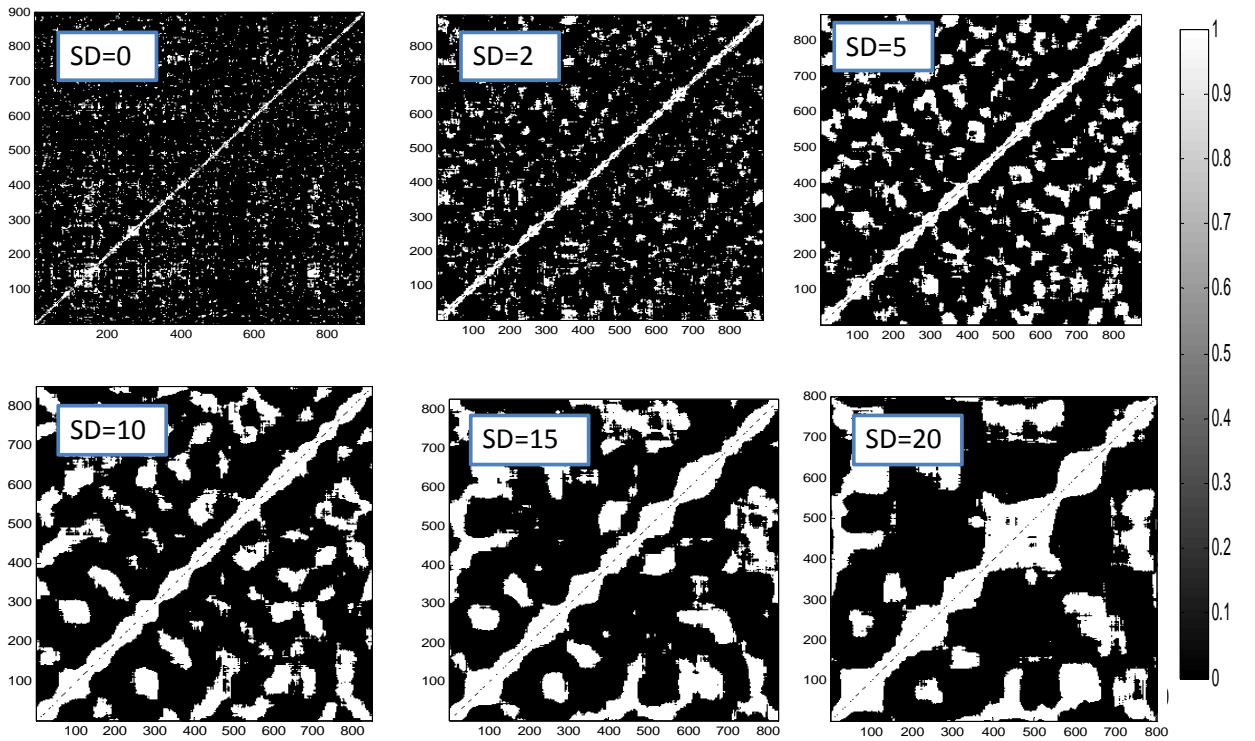
511 0,2,10 and 20 mm.

512



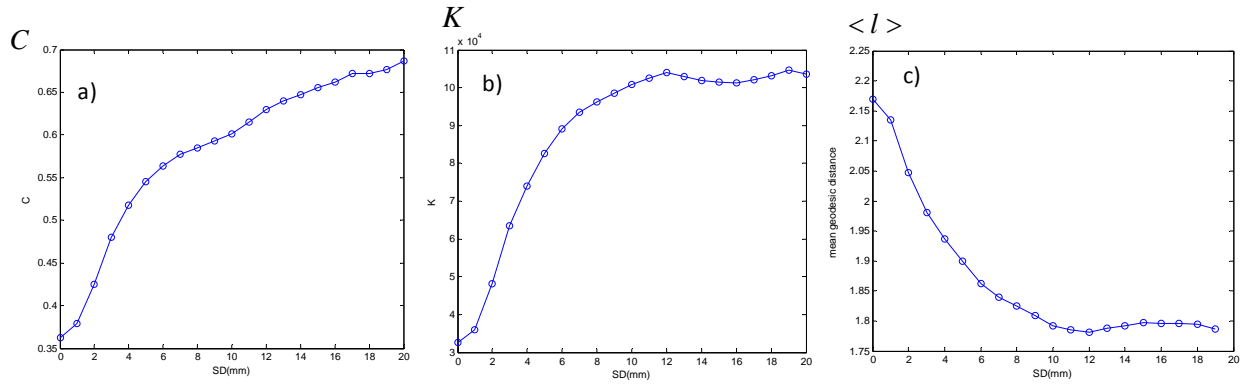
513

514 FIGURE 3. Correlation patterns throughout the shear displacements



515

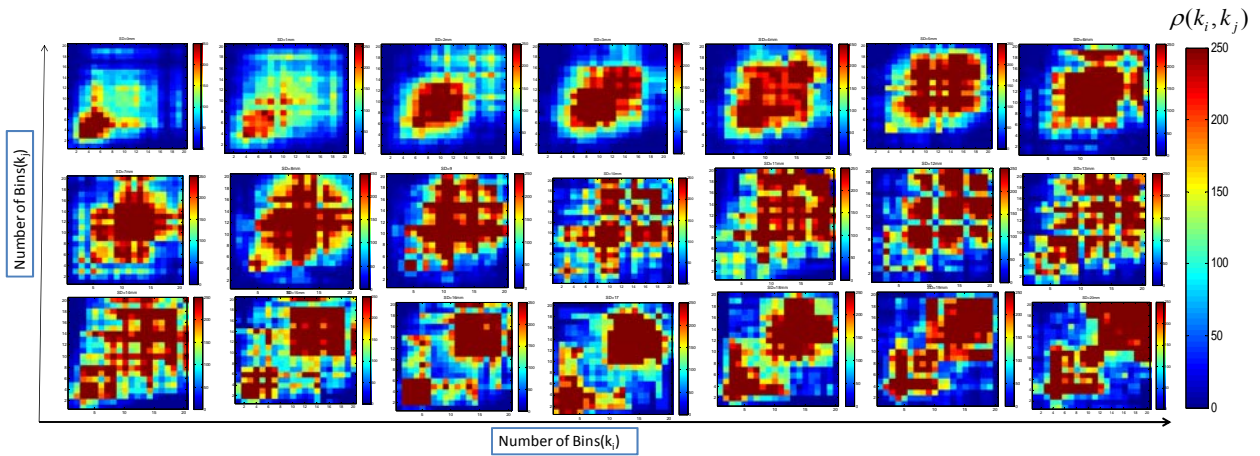
516 FIGURE 4. Visualization of adjacency matrix for the achieved networks



517

518 FIGURE 5. a) Clustering coefficient-Shear Displacement (SD), b) Number of edges-SD

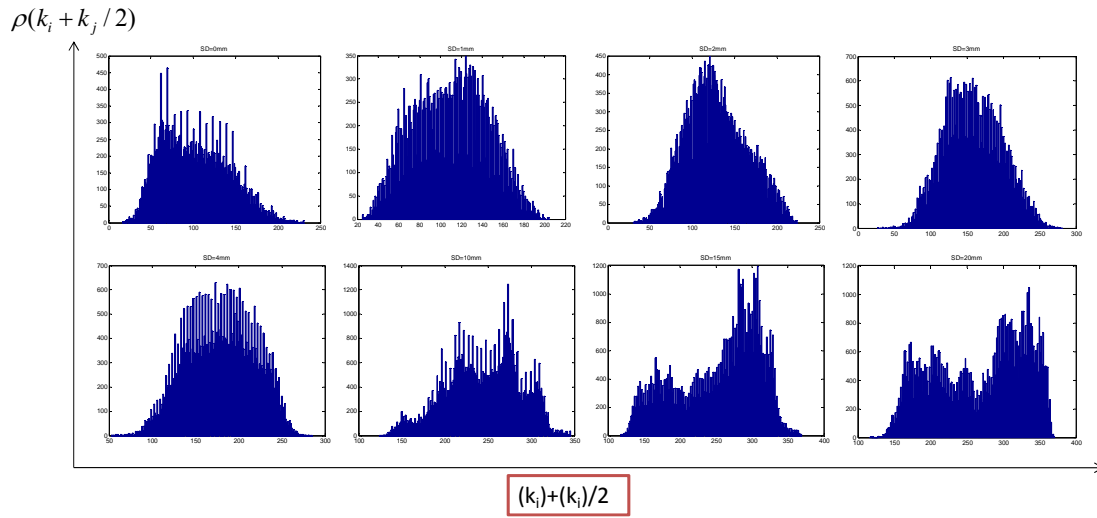
519 and c) Average path length-SD



520

521 FIGURE 6. Joint degree distribution from $SD=0$ to $SD=20$ mm (Top left-first row is

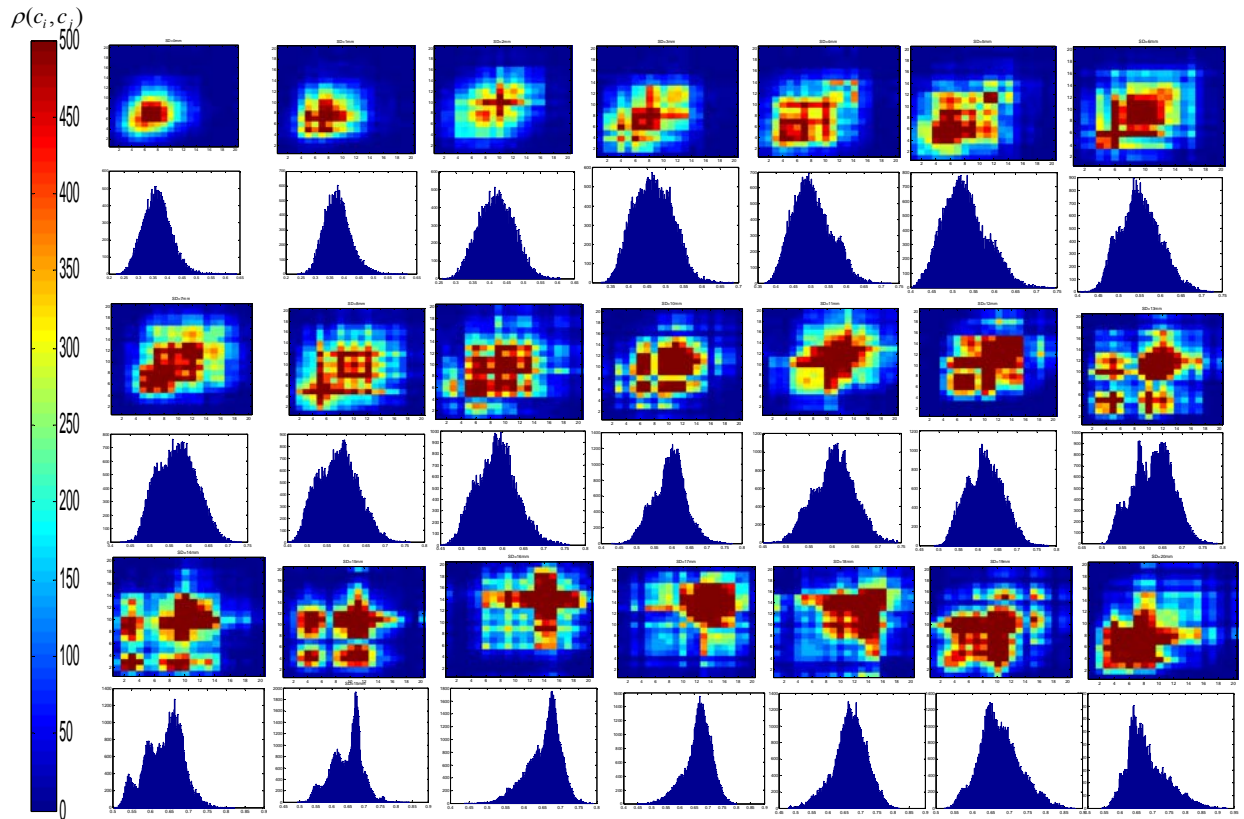
522 $SD=0$ and Top right -first row is 6mm shear slip)



523

524 FIGURE 7. Attributed weight distribution of links related to joint degree distribution

525 (for SD=0-4,10,15 and 20 mm)

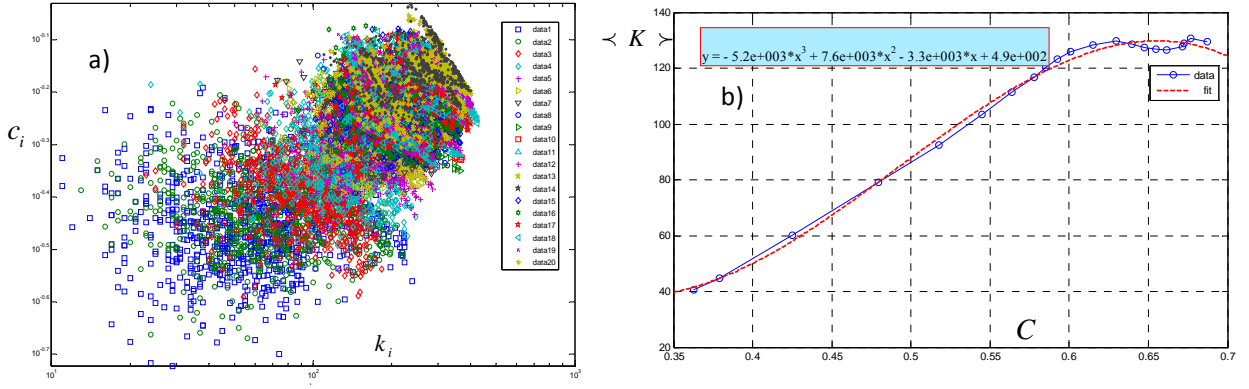


526

527 FIGURE 8. Joint clustering coefficient distribution plus attributed weight histograms
 528 based on averages of triangles connected to a link (sequence of figures are as well as
 529 figure 6).

530

531



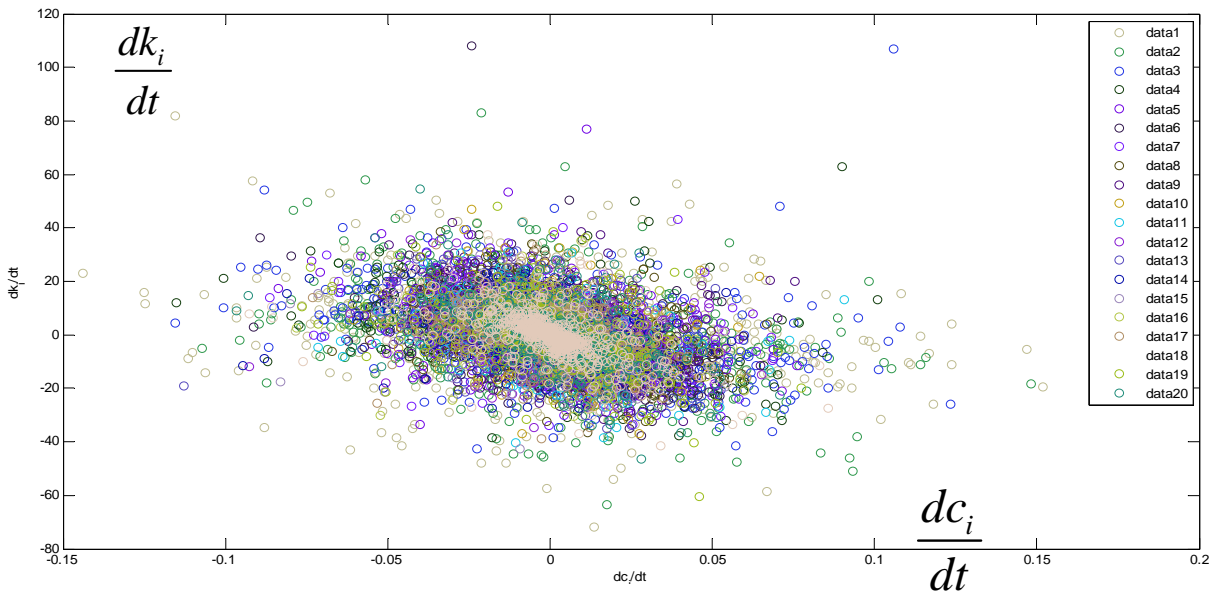
532

533 FIGURE 9. a) Spectrum of complex aperture networks ($c_i - k_i$) and b) Evolution of mean

534 degree of node against clustering coefficient and fitness of a polynomial function

535

536

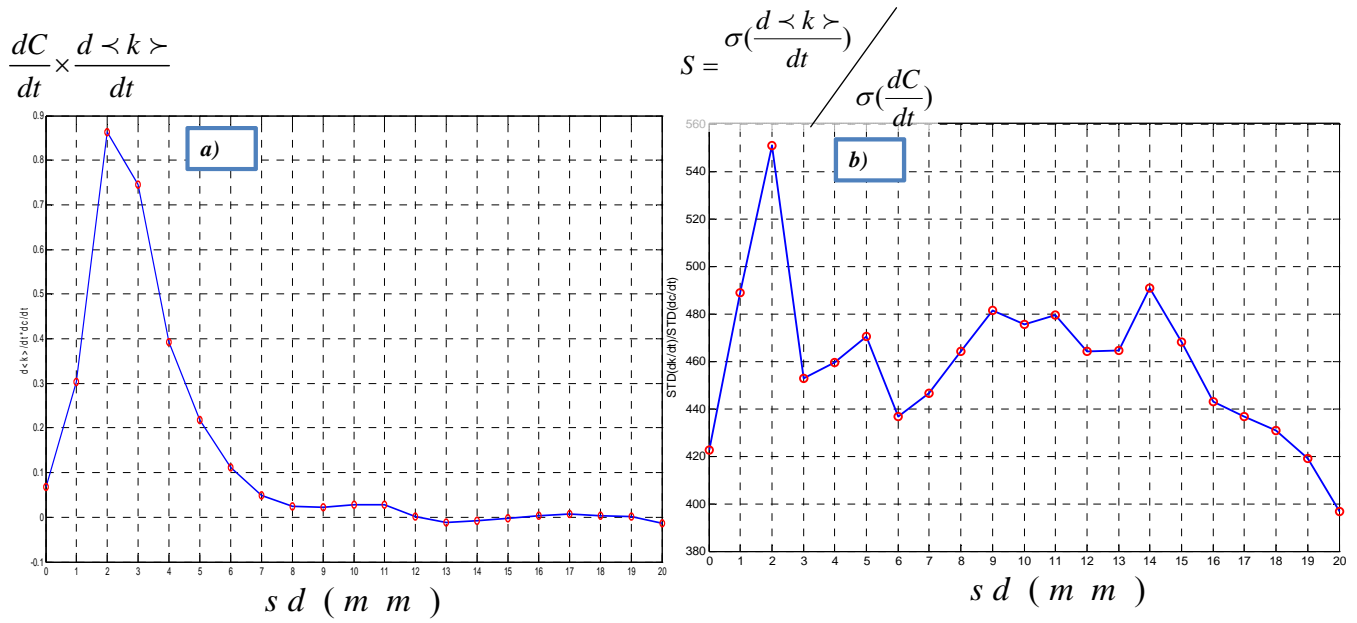


537

538 FIGURE 10. Data accumulation in $\frac{dk_i}{dt} - \frac{dc_i}{dt}$ space with respect to shear displacements

539 (data1 to data 20 are related to shear displacements from 0 to 20 mm).

540



541

542 FIGURE 11.a) Variation of $\frac{dC}{dt} \times \frac{d\langle k \rangle}{dt}$ with shear displacements and b) Anisotropy

543 evolution at the rate of spectrum (networks) space

544